Title

Multicomponent, multiphase interactions in fuel-cell inks

Authors

Berlinger, Sarah A

Garg, Samay

Weber, Adam Z

Publication Date

2021-10-01

DOI

10.1016/j.coelec.2021.100744

Peer reviewed

Available online at www.sciencedirect.com

ScienceDirect

Current Opinion in Electrochemistry

Review Article

Multicomponent, multiphase interactions in fuel-cell inks

Sarah A. Berlinger[1,2], Samay Garg[1,2] and Adam Z. Weber[1]

Abstract

Fuel-cell catalyst layers (CLs) are porous electrodes that are fabricated from CL inks: colloidal dispersions of catalyst particles and ion-conducting polymer (ionomer), dispersed in solvent(s). The complex interactions between the ink components ultimately dictate CL microstructure and electrochemical performance. To control the CL formation process and optimize fuel-cell performance, knowledge of these ink interactions is vital. In this review, we analyze data from ink-focused papers to elucidate how ink parameters (solvent type, ionomer-to-carbon ratio, etc.) impact ink interactions and CL performance. We then discuss these results in the context of the current understanding of two critical ink interactions: ionomer/solvent and ionomer/catalyst particle interactions.

Addresses

[1] Energy Conversion Group, Energy Technologies Area, Lawrence Berkeley National Laboratory, Berkeley, CA 94720, USA

[2] Department of Chemical & Biomolecular Engineering, University of California, Berkeley, Berkeley, CA 94720, USA

Corresponding author: Weber, Adam Z (azweber@lbl.gov)

Current Opinion in Electrochemistry 2021, **29**:100744

This review comes from a themed issue on **Fundamental and Theoretical Electrochemistry (2021)**

Edited by **Stephen Fletcher**

For complete overview about the section, refer Fundamental and Theoretical Electrochemistry (2021)

Available online 28 April 2021

https://doi.org/10.1016/j.coelec.2021.100744

Keywords

Fuel cells, Catalyst layers, Porous electrodes, Ink engineering, Ionomer, Colloidal interactions.

Introduction

The heart of proton-exchange-membrane fuel cells are their catalyst layers (CLs): heterogeneous porous electrodes composed of agglomerates of catalyst particles, ion-conducting polymer (ionomer), and void space. The ionomer serves both to bind the CL together and provide a pathway for ion transport [1,2]. Similarly, void space is crucial for gas and water transport, whereas the catalyst particles provide reaction sites and electron conduction pathways. These structures are necessarily complex, and characterization is nontrivial [3–5]. As such, there have been decades of research into CLs [1,6]. However, most studies have focused on relating structure to performance. Fundamental understanding of how those structures form is missing, with CL fabrication relying mostly on empiricism. This gap poses challenges for the community: if we are to engineer next-generation optimized CLs in an efficient manner, knowledge of how CL structures arise is crucial [7].

CLs are fabricated from inks that contain the catalyst particles and ionomer, dispersed in a solvent [7]. The particles and ionomer form agglomerates (on the order of 100s of nanometers) in the ink [1,6] that eventually determine the final CL microstructure. Important parameters that impact (or are impacted by) this ink-to-CL progression are shown in Figure 1. Ultimately, one desires to know how inputs (ink parameters) affect measurable outputs (CL parameters). Different ink parameters result in different interactions; these interactions modulate CL microstructure and performance. For example, the ionomer/solvent interaction controls the ionomer conformation in solution. The ionomer/particle interaction dictates how the ionomer adsorbs to the catalyst particles in the ink, modifying the ionomer/particle interface in the CL. Interactions between all three determine the agglomerate sizes and structures that self-assemble. Metrics of ink properties that reveal these different interactions are listed as interaction descriptors.

By understanding how ink parameters affect ink properties/interactions (which in turn dictate CL structure/performance), we can engineer inks to control and direct specific CL microstructures rather than rely on empirical and time-consuming optimization. With that goal in mind, this review is divided into two sections: first, a screening to understand how the ink parameters in Figure 1 impact ink and CL properties using literature data, and second, a discussion of the current state of understanding of two critical ink interactions (ionomer/

solvent and ionomer/particle) to help elucidate observed trends.

Ink parameter screening

Although there has been much CL research, the literature is full of contradictory data, partly because the properties or values of the ink parameter categories in Figure 1 (catalyst properties, ionomer chemistry, solvent type, and fabrication method) can be drastically different. Catalyst particles (on the order of a few nanometers) are usually platinum or platinum-alloy nanoparticles supported on larger carbon nanoparticles (although some efforts are focused on non−platinum group metal catalyst development [8−10]). The catalyst loading on the support particle can vary. Multiple carbon supports (~30−50 nm diameter) may be used: two common commercial types are Vulcan and high-surface-area carbon (HSC), although novel carbon supports are also explored [11−13]. Vulcan is more graphitic (and hydrophobic) than HSC. Because of Vulcan's low internal porosity, most platinum decorates the external surface in Vulcan-supported catalysts. In contrast, in HSC-supported catalysts, much platinum is located in internal pores. Furthermore, many ionomer chemistries are used. The most ubiquitous class of cation-conducting ionomers is perfluorosulfonic-acid (PFSA) ionomers, which consist of Teflon-like backbones and pendant sidechains that terminate in sulfonic-acid groups. However, even within PFSA chemistries, sidechain spacing (i.e. charge density, defined by the equivalent weight [EW], grams polymer/mole sulfonate) and length can differ; these alter the intrinsic ionomer properties [2]. Two commonly used ionomers are Nafion and Aquivion; Nafion possesses a longer sidechain (structures are shown in Supplementary Material Figure S1). Finally, the solvents used to disperse the ionomer and particles are not standardized: although alcohol−water mixtures are the most common, myriad others have been investigated [14]. In addition, even when considering the same solvent system, the composition may vary (i.e. the ratio of alcohol to water).

To complicate matters further beyond just material selection, fabrication choices can influence final properties. The method [15] and length of mixing [16] may differ. The ratio of components (namely, ionomer-to-

Figure 1

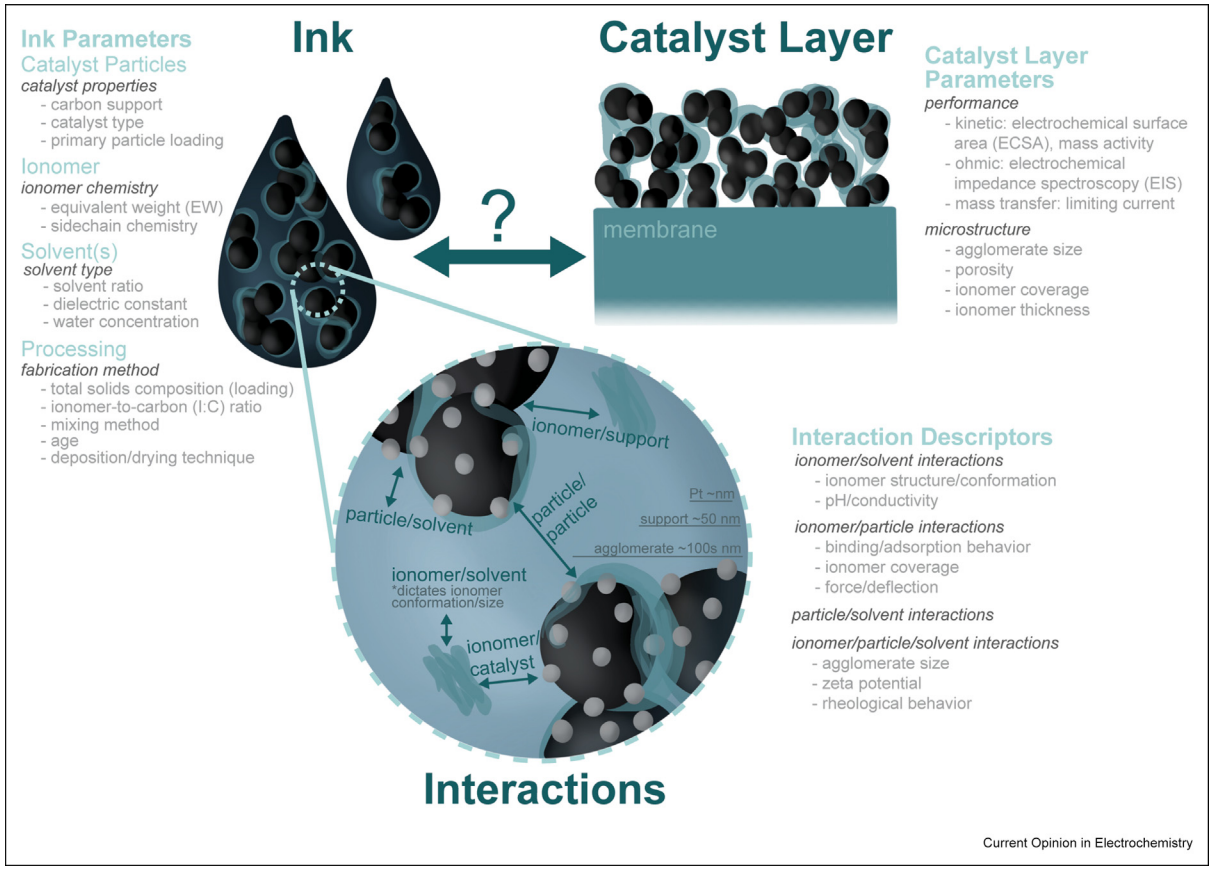

Pictorial representation of ink and catalyst layer structure (not meant to be exact or drawn to scale) and associated relevant important parameters that govern these structures/properties. Parameter list is not exhaustive. These parameters guided the database collection and regression analysis, as shown in Supplementary Material.

carbon [I:C] ratio) can be modified, as well as the total solids loading, which is often set by the deposition method: different techniques have different viscosity requirements. Ultrasonic-spray coating [17–19], doctor blading [20], screen printing [21], and roll-to-roll [22] processing of electrodes can occur either on the membrane to form a catalyst-coated membrane, on diffusion media to form a gas-diffusion electrode, or on a decal [23–25] and later transferred and hot pressed.

This disparate and massive parameter space makes it exceedingly difficult to compare studies directly to each other. In addition, within the literature, there are two main types of papers: CL focused and ink focused. Most papers fall into the former category and often report incomplete ink parameters, as their emphasis is on characterizing CL structure and performance. On the other hand, ink-focused papers systematically vary one ink parameter but typically investigate its impact on only one or two CL parameters. This yields collective information rich on either end of the ink-to-CL spectrum but lacks information connecting the two states. In an attempt to do so, we gathered data from ink-focused papers [19–21,24–42] that had sufficient detail about ink parameters listed in Figure 1 and performed a linear regression to test the correlation between these parameters and both ink interaction descriptors and CL parameters. To limit the scope, only papers using PFSA and platinum-based catalysts and those that investigated at least three variations of one parameter (i.e. three different solvents or I:C ratios, etc.) were chosen. Input parameters chosen for analysis were continuous variables (not discreet) that were consistently reported, and output variables were chosen based on the prevalence of data available. From these criteria, we selected I:C ratio, solvent dielectric constant (ε), zeta potential, agglomerate size, electrochemical surface area (ECSA), and limiting current density (i_{lim}) as variables to perform the regression. More details on data collection/analysis, additional parameter plots, the full database, and parameter selection (listed in Table S1) can be found in Supplementary Material.

Figure 2 examines the influence of ε on interaction descriptors (agglomerate diameter and zeta potential) and CL parameters (i_{lim} and ECSA). Because a wide range of solvents and solvent mixtures have been explored, solvent is represented by ε to easily compare across different studies. Figure 3 plots the same properties, now as a function of I:C ratio. The first thing to note is that no parameter of the ones studied is controlling; there are certainly correlations, but outcomes cannot be predicted solely from one parameter. Spread in the data is because of the variability in all the other ink parameters. In addition, particularly for the I:C ratio data, there are clusters of points located at one value (i.e. I:C ratio of 1); variability in the y-value is again because of the differences in the other parameters not held constant. That

Figure 2

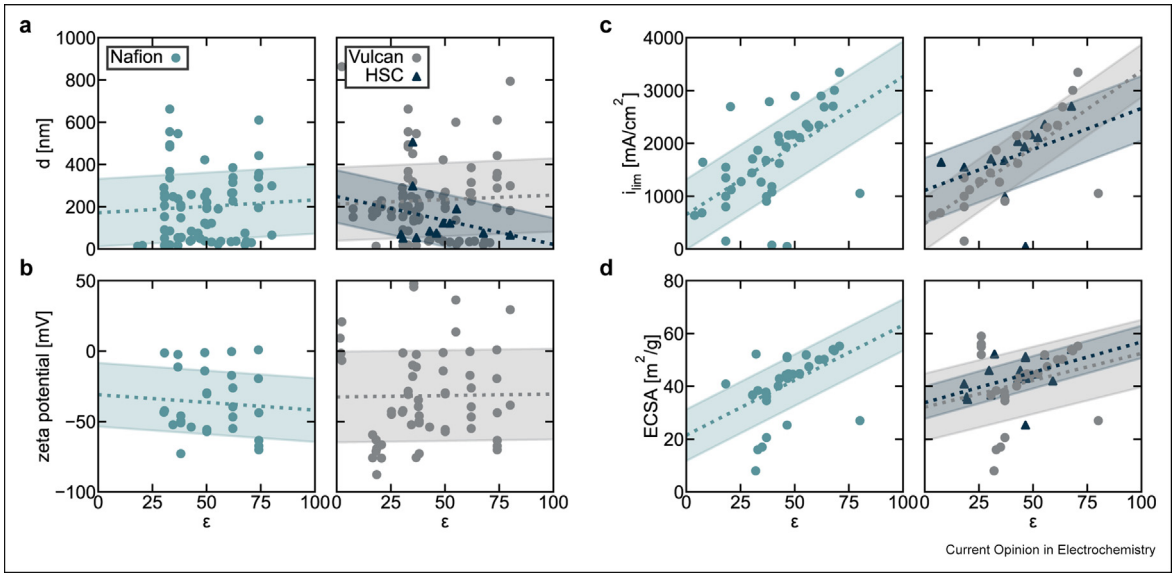

Data from Refs. [19–21,24–42] that displays the effect solvent dielectric constant (ε) has on (**a, b**) ink interaction descriptors (agglomerate diameter, d, and zeta potential) and (**c, d**) catalyst layer parameters (limiting current density, i_{lim}, and electrochemical surface area [ECSA]). The left and right panels of each subplot categorize similar data based on ionomer type (left) or carbon support type (right). The shaded region represents one standard error of the regression fit (dotted line).

being said, a few general trends are observed. First, there is no strong correlation between agglomerate diameter and zeta potential as a function of ε, suggesting that the primary forces controlling the aggregation process are not electrostatic in nature. However, CL performance does seem to be related to ε: Figure 2 shows ECSA and i_{lim} increasing with ε. This is in agreement with recent studies that demonstrated the impact of water:propanol ratio on CL performance and ionomer agglomerate coverage [19].

In Figure 3, we see zeta potential generally becomes more negatives as I:C ratio increases, likely because of greater ionomer adsorption to the agglomerate surface. We also see CL parameters are impacted by I:C ratio, which has been the focus of a number of studies [21,41,43,44]. Electrochemical performance is controlled by how much ionomer is in contact with the catalyst sites: too much results in high transport resistances and catalyst poisoning, whereas too little ionomer coverage yields insufficient ion conduction [45–50]. The lack of consensus on an optimal I:C ratio value indicates that it is material dependent; this is evidenced by the different I:C ratio trends for HSC and Vulcan in Figure 3. Most probably, optimal I:C ratio also depends on parameters such as solvent, EW, etc. Although these trends are complex, it is clear solvent choice and I:C ratio alter ink interactions and CL parameters.

Ionomer/solvent interactions

Because molecular weight distributions are difficult to characterize for PFSAs, most PFSA dispersion analysis has relied on characterizing aggregate structure; the PFSA dispersing solvent affects its conformation. Scattering [14,51,52] and molecular dynamics (MD) simulations [53–56] reveal that in many polar solvents, PFSA forms cylindrical bundles, although swollen spheres and random coils have also been observed. This solvent-induced conformation is driven by competing preferences for hydrophobic backbone aggregation and electrostatic sidechain repulsion. The solvent/ionomer interaction has been described using solubility parameters that have been measured for both the backbone and the sidechains [29].

As mentioned earlier, water–alcohol mixtures are some of the most commonly studied solvents. Changing the water:propanol ratio changes the relative acidity of the dispersions, which is hypothesized to be because of sidechain/solvent versus backbone/solvent interactions [26]. Namely, the sidechains of PFSA may preferentially extend outward into solution in water-rich solvents, whereas in propanol-rich solvents, PFSA conformation may have a more hydrophobic exterior. Similar structures were predicted using MD simulations; by explicitly considering both solvents, it is shown that different solvents partition inside versus outside the PFSA aggregate [56].

Figure 3

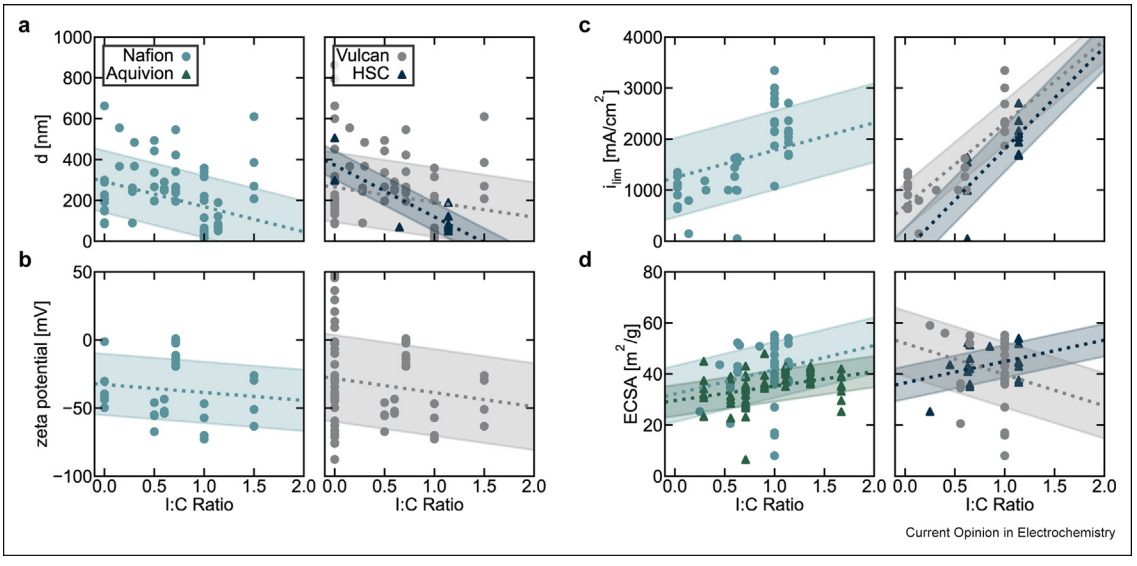

Data from Refs. [19–21,24–42] that displays the effect ionomer-to-carbon (I:C) ratio has on (**a, b**) ink interaction descriptors (agglomerate diameter, d, and zeta potential) and (**c, d**) catalyst layer parameters (limiting current density, i_{lim}, and electrochemical surface area [ECSA]). The left and right panels of each subplot categorize similar data based on ionomer type (left) or carbon support type (right). The shaded region represents one standard error of the regression fit (dotted line).

These dispersion conformations modulate the properties of films and membranes once cast [57–60]. *In situ* scattering was recently used to understand the dispersion-to-film transition and how different solvents determine the evolution of thin-film morphology during drying [60,61]. Conductivity and water uptake measurements show that as the water content in the dispersion increases relative to propanol, the transport properties of the cast film improve [60]. It is possible the enhanced i_{lim} in Figure 2 at higher ε could in part be because of this effect.

The fact that solvent type alters the final structure and properties of thin films has additional implications. PFSA used in ink formulations and thin-film studies is often diluted from stock dispersions that come in various different solvents themselves. One must consider both the solvent used to dilute (i.e. the ink solvent) as well as the native stock solvent, as these will both alter PFSA behavior.

Finally, these different dispersion conformations (aggregate size, degree of hydrophilicity/hydrophobicity, etc.) will influence how the ionomer adsorbs to catalyst particles in solution (altering the ionomer/particle interaction, discussed in the next section). Modified Derjaguin-Landau-Verwey-Overbeek (DLVO) theory has been applied to ink systems to try to understand aggregation processes [30,62]. Although these are important first steps in modeling ink interactions, they overlook some important physics. In DLVO theory, solvent modifies the Hamaker attraction term and the electrostatic repulsion potential through changes in ε. However, in addition to changing ε, solvent alters the physical characteristics of the PFSA aggregate, as discussed previously. Both these effects will influence overall aggregation behavior, and the coupling between them cannot be ignored. Figure 2 demonstrates this point: solvent ε definitively changes CL performance, but the aggregation process is not governed by classical (electrostatic) DLVO forces (exemplified by the aggregate size and zeta potential trends).

Ionomer/particle interactions

The ionomer/particle interaction encompasses both the ionomer/platinum and the ionomer/support (carbon) interaction. Let us first consider the ionomer/carbon interaction. MD simulations have shown that PFSA interacts with carbon surfaces via backbone adsorption [63,64]; this interaction is likely hydrophobic in nature [63]. Importantly, adsorption was predicted to be a strong function of solvent environment and EW [64]. This was recently verified experimentally by quartz crystal microbalance experiments [65]. In addition, PFSA binding behavior to carbon has been probed with isothermal titration calorimetry; the analysis of the entropic and enthalpic contributions to the binding free energy reveals that the binding process is entropically dominated [65,66]. This also points to hydrophobic interactions between PFSA and the carbon surface.

Because the ionomer/platinum interface controls electrochemical reactions, the ionomer/platinum interaction has received much attention in the literature. During fuel cell operation, many groups have noted that the PFSA sulfonate moieties interact with the platinum catalyst surface, effectively poisoning the catalyst by blocking active sites [49,50,67–69]. This is also evidenced by increased oxygen transport resistance [45,70]. A number of groups have extrapolated the results of these *operando* studies and have assumed there is a strong, inherent platinum/sulfonate interaction; they postulate this interaction drives adsorption to agglomerates in the ink. However, it is important to note that this interaction is potential dependent and primarily noted at elevated potentials [67] (above the potential of zero charge [71,72]). In addition, spectroscopic studies have shown that in addition to sulfonate groups, there is co-adsorption of fluorocarbon [67,68,73] and ether oxygen groups [50]. In inks, while binding strength does increase with decreasing EW, the amount of PFSA that adsorbs to platinum is less than the amount that adsorbs to a hydrophobic (carbon-like) surface [65]. Moreover, the binding mechanism is entropically driven, similar to that seen with carbon [65].

All previously mentioned information suggests that the ionomer/platinum ink interaction is different from that in operating fuel cells: in inks, it is not particularly strong, compared with the other interactions present. Although *ex situ* thin-film studies have revealed different behavior on platinum surfaces versus on silicon [74,75], it is possible this is merely because of changes in substrate hydrophobicity, rather than because of strong specific-ion binding between sulfonate and platinum. In fact, PFSA structures have been shown to order differently on substrates of varying hydrophobicity [76]. These ionomer/platinum ink interactions are also subject to dispersion solvent effects: atomic force microscopy studies reveal that PFSA films are smoother when they adsorb from mixed water-propanol solvents onto platinum, rather than from high-water concentration solvents [73].

Given the differences (and similarities) between the ionomer/platinum and ionomer/carbon ink interaction, and because of the larger surface area of carbon relative to platinum on the exterior of catalyst particles, it is likely that solution-level interactions are primarily controlled by ionomer/carbon interactions. This indicates that different carbon types should manifest different ionomer/carbon interactions; the impact this has on CL performance should be evident when exploring I:C ratio. This is seen in Figure 3: parameters

have different trends as a function of I:C when using Vulcan versus HSC.

Concluding remarks

Ultimately, the goal is to be able to predict CL performance, given certain ink parameters, or even better, be able to determine how an ink would need to change to achieve optimal CL performance via optimized structure. That way, if a more active catalyst type is created, or a more conductive and stable ionomer is synthesized, one could know *a priori* how it would affect CL properties, without the need for months of empirical optimization. To make this a reality, we must understand how ink parameters impact ink interactions (and interaction descriptors) and, in turn, how these interactions dictate CL parameters. However, because of disparate material sets used and often incomplete experimental methods detailing CL fabrication, it is difficult to make use of the wealth of CL literature. Rather, systematic, ink-focused research is needed, and the community must make a concerted effort to report all relevant ink details (i.e. metadata) moving forward.

Despite these challenges, great strides have been made toward understanding how ink parameters influence ink interactions, in particular, ionomer/particle and ionomer/solvent interactions. Next, it is imperative to link interaction descriptors to CL parameters. In this way, we can completely understand (and therefore control) the ink-to-CL fabrication process, enabling ink engineering for smarter CL design.

Declaration of competing interest

The authors declare that they have no known competing financial interests or personal relationships that could have appeared to influence the work reported in this paper.

Acknowledgements

The authors would like to thank Dr. Ahmet Kusoglu and Ms. Anamika Chowdhury for helpful discussions. This material is based on work performed by the Million Mile Fuel Cell Truck (M2FCT) Consortium (https://millionmilefuelcelltruck.org), technology manager Greg Kleen, which is supported by the U.S. Department of Energy, Office of Energy Efficiency and Renewable Energy, Hydrogen and Fuel Cell Technologies Office, under contract numbers DE-AC02-05CH11231.

Appendix A. Supplementary data

Supplementary data to this article can be found online at https://doi.org/10.1016/j.coelec.2021.100744.

References

Papers of particular interest, published within the period of review, have been highlighted as:

* of special interest
** of outstanding interest

1. Holdcroft S: **Fuel cell catalyst layers: a polymer science perspective**. *Chem Mater* 2014, **26**:381–393, https://doi.org/10.1021/cm401445h.

2. * Kusoglu A, Weber AZ: **New insights into perfluorinated sulfonic-acid ionomers**. *Chem Rev* 2017, **117**:987–1104, https://doi.org/10.1021/acs.chemrev.6b00159.
Extremely comprehensive review detailing PFSA ionomers, with a particular emphasis on membrane and thin film properties.

3. Cetinbas FC, Ahluwalia RK, Kariuki NN, Myers DJ: **Agglomerates in polymer electrolyte fuel cell electrodes: Part I. Structural characterization**. *J Electrochem Soc* 2018, **165**:F1051–F1058, https://doi.org/10.1149/2.0571813jes.

4. Epting WK, Gelb J, Litster S: **Resolving the three-dimensional microstructure of polymer electrolyte fuel cell electrodes using nanometer-scale X-ray computed tomography**. *Adv Funct Mater* 2012, **22**:555–560, https://doi.org/10.1002/adfm.201101525.

5. Cullen DA, Koestner R, Kukreja RS, Liu ZY, Minko S, Trotsenko O, Tokarev A, Guetaz L, Meyer HM, Parish CM, *et al.*: **Imaging and microanalysis of thin ionomer layers by scanning transmission electron microscopy**. *J Electrochem Soc* 2014, **161**:F1111–F1117, https://doi.org/10.1149/2.1091410jes.

6. Karan K: **PEFC catalyst layer: recent advances in materials, microstructural characterization, and modeling**. *Curr Opin Electrochem* 2017, **5**:27–35, https://doi.org/10.1016/j.coelec.2017.08.018.

7. Hatzell KB, Dixit MB, Berlinger SA, Weber AZ: **Understanding inks for porous-electrode formation**. *J Mater Chem A* 2017, **5**:20527–20533, https://doi.org/10.1039/C7TA07255D.

8. Thompson ST, Wilson AR, Zelenay P, Myers DJ, More KL, Neyerlin KC, Papageorgopoulos D: **ElectroCat: DOE's approach to PGM-free catalyst and electrode R&D**. *Solid State Ionics* 2018, **319**:68–76, https://doi.org/10.1016/j.ssi.2018.01.030.

9. Serov A, Artyushkova K, Niangar E, Wang C, Dale N, Jaouen F, Sougrati M-T, Jia Q, Mukerjee S, Atanassov P: **Nano-structured non-platinum catalysts for automotive fuel cell application**. *Nano Energy* 2015, **16**:293–300, https://doi.org/10.1016/j.nanoen.2015.07.002.

10. Shao Y, Dodelet J-P, Wu G, Zelenay P: **PGM-free cathode catalysts for PEM fuel cells: a mini-review on stability challenges**. *Adv Mater* 2019, **31**:1807615, https://doi.org/10.1002/adma.201807615.

11. Antolini E: **Carbon supports for low-temperature fuel cell catalysts**. *Appl Catal B Environ* 2009, **88**:1–24, https://doi.org/10.1016/j.apcatb.2008.09.030.

12. Yarlagadda V, Carpenter MK, Moylan TE, Kukreja RS, Koestner R, Gu W, Thompson L, Kongkanand A: **Boosting fuel cell performance with accessible carbon mesopores**. *ACS Energy Lett* 2018, **3**:618–621, https://doi.org/10.1021/acsenergylett.8b00186.

13. Samad S, Loh KS, Wong WY, Lee TK, Sunarso J, Chong ST, Wan Daud WR: **Carbon and non-carbon support materials for platinum-based catalysts in fuel cells**. *Int J Hydrogen Energy* 2018, **43**:7823–7854, https://doi.org/10.1016/j.ijhydene.2018.02.154.

14. ** Welch C, Labouriau A, Hjelm R, Orler B, Johnston C, Kim YS: **Nafion in dilute solvent systems: dispersion or solution?** *ACS Macro Lett* 2012, **1**:1403–1407, https://doi.org/10.1021/mz3005204.
Small-angle neutron studies reveal how ionomer solution conformation is drastically affected by solvent identity.

15. Du S, Li W, Wu H, Abel Chuang P-Y, Pan M, Sui P-C: **Effects of ionomer and dispersion methods on rheological behavior of proton exchange membrane fuel cell catalyst layer ink**. *Int J Hydrogen Energy* 2020, **45**:29430–29441, https://doi.org/10.1016/j.ijhydene.2020.07.241.

16. Wang M, Park JH, Kabir S, Neyerlin KC, Kariuki NN, Lv H, Stamenkovic VR, Myers DJ, Ulsh M, Mauger SA: **Impact of catalyst ink dispersing methodology on fuel cell performance using in-situ X-ray scattering**. *ACS Appl Energy Mater* 2019, **2**:6417–6427, https://doi.org/10.1021/acsaem.9b01037.

17. Mauger SA, Pfeilsticker JR, Wang M, Medina S, Yang-Neyerlin AC, Neyerlin KC, Stetson C, Pylypenko S, Ulsh M:

Fabrication of high-performance gas-diffusion-electrode based membrane-electrode assemblies. *J Power Sources* 2020, **450**:227581, https://doi.org/10.1016/j.jpowsour.2019.227581.

18. Millington B, Whipple V, Pollet BG: **A novel method for preparing proton exchange membrane fuel cell electrodes by the ultrasonic-spray technique**. *J Power Sources* 2011, **196**: 8500–8508, https://doi.org/10.1016/j.jpowsour.2011.06.024.

19. ** Van Cleve T, Khandavalli S, Chowdhury A, Medina S, Pylypenko S, Wang M, More KL, Kariuki NN, Myers DJ, Weber AZ, *et al.*: **Dictating Pt-based electrocatalyst performance in polymer electrolyte fuel cells; from formulation to application**. *ACS Appl Mater Interfaces* 2019, **11**:46953–46964, https://doi.org/10.1021/acsami.9b17614.
Demonstrates the effect of varying ink water:propanol ratios on ink properties and how this affects fuel cell performance. The authors quantify both electrochemical performance (polarization curves) and morphological features (ionomer coverage).

20. Huang DC, Yu PJ, Liu FJ, Huang SL, Hsueh KL, Chen YC, Wu CH, Chang WC, Tsau FH: **Effect of dispersion solvent in catalyst ink on proton exchange membrane fuel cell performance**. *Int J Electrochem Sci* 2011, **6**:2551–2565.

21. Alink R, Singh R, Schneider P, Christmann K, Schall J, Keding R, Zamel N: **Full parametric study of the influence of ionomer content, catalyst loading and catalyst type on oxygen and ion transport in PEM fuel cell catalyst layers**. *Molecules* 2020, **25**: 1523, https://doi.org/10.3390/molecules25071523.

22. Mauger SA, Neyerlin KC, Yang-Neyerlin AC, More KL, Ulsh M: **Gravure coating for roll-to-roll manufacturing of proton-exchange-membrane fuel cell catalyst layers**. *J Electrochem Soc* 2018, **165**:F1012–F1018, https://doi.org/10.1149/2.0091813jes.

23. Saha MS, Paul DK, Peppley BA, Karan K: **Fabrication of catalyst-coated membrane by modified decal transfer technique**. *Electrochem Commun* 2010, **12**:410–413, https://doi.org/10.1016/j.elecom.2010.01.006.

24. Orfanidi A, Rheinländer PJ, Schulte N, Gasteiger HA: **Ink solvent dependence of the ionomer distribution in the catalyst layer of a PEMFC**. *J Electrochem Soc* 2018, **165**:F1254–F1263, https://doi.org/10.1149/2.1251814jes.

25. Suzuki T, Tsushima S, Hirai S: **Effects of Nafion® ionomer and carbon particles on structure formation in a proton-exchange membrane fuel cell catalyst layer fabricated by the decal-transfer method**. *Int J Hydrogen Energy* 2011, **36**:12361–12369, https://doi.org/10.1016/j.ijhydene.2011.06.090.

26. * Berlinger SA, McCloskey BD, Weber AZ: **Inherent acidity of perfluorosulfonic acid ionomer dispersions and implications for ink aggregation**. *J Phys Chem B* 2018, **122**:7790–7796, https://doi.org/10.1021/acs.jpcb.8b06493.
The authors show that the acidity of PFSA dispersions increases as ink water:propanol ratio increases, and this pH change may be a proxy for conformational change. This has important implications for electrostatic and hydrophobic interactions between PFSA and other ink components.

27. ** Khandavalli S, Park JH, Kariuki NN, Myers DJ, Stickel JJ, Hurst K, Neyerlin KC, Ulsh M, Mauger SA: **Rheological investigation on the microstructure of fuel cell catalyst inks**. *ACS Appl Mater Interfaces* 2018, **10**:43610–43622, https://doi.org/10.1021/acsami.8b15039.
Uses rheology to probe interactions between ionomer and particles in inks for fixed solvent ratio. The authors examine the influence of carbon support type (Vulcan versus HSC) and I:C ratio.

28. Balu R, Choudhury NR, Mata JP, de Campo L, Rehm C, Hill AJ, Dutta NK: **Evolution of the interfacial structure of a catalyst ink with the quality of the dispersing solvent: a contrast variation small-angle and ultrasmall-angle neutron scattering investigation**. *ACS Appl Mater Interfaces* 2019, **11**:9934–9946, https://doi.org/10.1021/acsami.8b20645.

29. Ngo TT, Yu TL, Lin H-L: **Influence of the composition of isopropyl alcohol/water mixture solvents in catalyst ink solutions on proton exchange membrane fuel cell performance**. *J Power Sources* 2013, **225**:293–303, https://doi.org/10.1016/j.jpowsour.2012.10.055.

30. * Dixit MB, Harkey BA, Shen F, Hatzell KB: **Catalyst layer ink interactions that affect coatability**. *J Electrochem Soc* 2018, **165**:F264–F271, https://doi.org/10.1149/2.0191805jes.
The authors use a variety of techniques, including dynamic light scattering, rheology, and surface tension measurements, to understand the impact of solvent and I/C ratio on ink properties. They model their results with extended DLVO theory.

31. Jung C-Y, Kim W-J, Yi S-C: **Optimization of catalyst ink composition for the preparation of a membrane electrode assembly in a proton exchange membrane fuel cell using the decal transfer**. *Int J Hydrogen Energy* 2012, **37**:18446–18454, https://doi.org/10.1016/j.ijhydene.2012.09.013.

32. Kim T-H, Yi J-Y, Jung C-Y, Jeong E, Yi S-C: **Solvent effect on the Nafion agglomerate morphology in the catalyst layer of the proton exchange membrane fuel cells**. *Int J Hydrogen Energy* 2017, **42**:478–485, https://doi.org/10.1016/j.ijhydene.2016.12.015.

33. Millington B, Du S, Pollet BG: **The effect of materials on proton exchange membrane fuel cell electrode performance**. *J Power Sources* 2011, **196**:9013–9017, https://doi.org/10.1016/j.jpowsour.2010.12.043.

34. Thanasilp S, Hunsom M: **Effect of MEA fabrication techniques on the cell performance of Pt–Pd/C electrocatalyst for oxygen reduction in PEM fuel cell**. *Fuel* 2010, **89**:3847–3852, https://doi.org/10.1016/j.fuel.2010.07.008.

35. Therdthianwong A, Ekdharmasuit P, Therdthianwong S: **Fabrication and performance of membrane electrode assembly prepared by a catalyst-coated membrane method: effect of solvents used in a catalyst ink mixture**. *Energy Fuels* 2010, **24**: 1191–1196, https://doi.org/10.1021/ef901105k.

36. Yang F, Xin L, Uzunoglu A, Qiu Y, Stanciu L, Ilavsky J, Li W, Xie J: **Investigation of the interaction between Nafion ionomer and surface functionalized carbon black using both ultrasmall angle X-ray scattering and Cryo-TEM**. *ACS Appl Mater Interfaces* 2017, **9**:6530–6538, https://doi.org/10.1021/acsami.6b12949.

37. Orfanidi A, Madkikar P, El-Sayed HA, Harzer GS, Kratky T, Gasteiger HA: **The key to high performance low Pt loaded electrodes**. *J Electrochem Soc* 2017, **164**:F418–F426, https://doi.org/10.1149/2.1621704jes.

38. Xu R, Wu C, Xu H: **Particle size and zeta potential of carbon black in liquid media**. *Carbon* 2007, **45**:2806–2809, https://doi.org/10.1016/j.carbon.2007.09.010.

39. Doo G, Lee JH, Yuk S, Choi S, Lee D-H, Lee DW, Kim HG, Kwon SH, Lee SG, Kim H-T: **Tuning the ionomer distribution in the fuel cell catalyst layer with scaling the ionomer aggregate size in dispersion**. *ACS Appl Mater Interfaces* 2018, **10**: 17835–17841, https://doi.org/10.1021/acsami.8b01751.

40. Ngo TT, Yu TL, Lin H-L: **Nafion-based membrane electrode assemblies prepared from catalyst inks containing alcohol/water solvent mixtures**. *J Power Sources* 2013, **238**:1–10, https://doi.org/10.1016/j.jpowsour.2013.03.055.

41. Sasikumar G, Ihm JW, Ryu H: **Optimum Nafion content in PEM fuel cell electrodes**. *Electrochim Acta* 2004, **50**:601–605, https://doi.org/10.1016/j.electacta.2004.01.126.

42. Sasikumar G, Ihm JW, Ryu H: **Dependence of optimum Nafion content in catalyst layer on platinum loading**. *J Power Sources* 2004, **132**:11–17, https://doi.org/10.1016/j.jpowsour.2003.12.060.

43. Passalacqua E, Lufrano F, Squadrito G, Patti A, Giorgi L: **Nafion content in the catalyst layer of polymer electrolyte fuel cells: effects on structure and performance**. *Electrochim Acta* 2001, **46**:799–805, https://doi.org/10.1016/S0013-4686(00)00679-4.

44. Ishikawa H, Sugawara Y, Inoue G, Kawase M: **Effects of Pt and ionomer ratios on the structure of catalyst layer: a theoretical model for polymer electrolyte fuel cells**. *J Power Sources*

2018, **374**:196–204, https://doi.org/10.1016/j.jpowsour.2017.11.026.

45. Weber AZ, Kusoglu A: **Unexplained transport resistances for low-loaded fuel-cell catalyst layers**. *J Mater Chem A* 2014, **2**: 17207–17211, https://doi.org/10.1039/C4TA02952F.

46. Kongkanand A, Mathias MF: **The priority and challenge of high-power performance of low-platinum proton-exchange membrane fuel cells**. *J Phys Chem Lett* 2016, **7**:1127–1137, https://doi.org/10.1021/acs.jpclett.6b00216.

47. Schuler T, Chowdhury A, Freiberg AT, Sneed B, Spingler FB, Tucker MC, More KL, Radke CJ, Weber AZ: **Fuel-cell catalyst-layer resistance via hydrogen limiting-current measurements**. *J Electrochem Soc* 2019, **166**:F3020–F3031, https://doi.org/10.1149/2.0031907jes.

48. Sadeghi E, Putz A, Eikerling M: **Effects of ionomer coverage on agglomerate effectiveness in catalyst layers of polymer electrolyte fuel cells**. *J Solid State Electrochem* 2014, **18**: 1271–1279, https://doi.org/10.1007/s10008-013-2268-z.

49. Subbaraman R, Strmcnik D, Stamenkovic V, Markovic NM: **Three phase interfaces at electrified metal–solid electrolyte systems 1. Study of the Pt(hkl)–Nafion interface**. *J Phys Chem C* 2010, **114**:8414–8422, https://doi.org/10.1021/jp100814x.

50. Kodama K, Motobayashi K, Shinohara A, Hasegawa N, Kudo K, Jinnouchi R, Osawa M, Morimoto Y: **Effect of the side-chain structure of perfluoro-sulfonic acid ionomers on the oxygen reduction reaction on the surface of Pt**. *ACS Catal* 2018, **8**: 694–700, https://doi.org/10.1021/acscatal.7b03571.

51. Loppinet B, Gebel G: **Rodlike colloidal structure of short pendant chain perfluorinated ionomer solutions**. *Langmuir* 1998, **14**:1977–1983, https://doi.org/10.1021/la9710987.

52. Loppinet B, Gebel G, Williams CE: **Small-angle scattering study of perfluorosulfonated ionomer solutions**. *J Phys Chem B* 1997, **101**:1884–1892, https://doi.org/10.1021/jp9623047.

53. Mabuchi T, Huang S-F, Tokumasu T: **Dispersion of Nafion ionomer aggregates in 1-propanol/water solutions: effects of ionomer concentration, alcohol content, and salt addition**. *Macromolecules* 2020, **53**:3273–3283, https://doi.org/10.1021/acs.macromol.9b02725.

54. Kuo A-T, Urata S, Nakabayashi K, Watabe H, Honmura S: **Coarse-grained molecular dynamics simulation of perfluorosulfonic acid polymer in water–ethanol mixtures**. *Macromolecules* 2021, **54**:609–620, https://doi.org/10.1021/acs.macromol.0c02364.

55. Ghelichi M, Malek K, Eikerling MH: **Ionomer self-assembly in dilute solution studied by coarse-grained molecular dynamics**. *Macromolecules* 2016, **49**:1479–1489, https://doi.org/10.1021/acs.macromol.5b02158.

56. ** Tarokh A, Karan K, Ponnurangam S: **Atomistic MD study of Nafion dispersions: role of solvent and counterion in the aggregate structure, ionic clustering, and acid dissociation**. *Macromolecules* 2020, **53**:288–301, https://doi.org/10.1021/acs.macromol.9b01663.
Builds on previous molecular dynamics simulations by explicitly considering solvent(s) molecules. The authors detail an ionomer conformation phase diagram across a wide range of dielectric constant solvents studied, showing three main classes of aggregate structures, and solvent partitioning inside versus outside the ionomer aggregate.

57. Lin H-L, Yu TL, Huang C-H, Lin T-L: **Morphology study of Nafion membranes prepared by solutions casting**. *J Polym Sci B Polym Phys* 2005, **43**:3044–3057, https://doi.org/10.1002/polb.20599.

58. Ma C-H, Yu TL, Lin H-L, Huang Y-T, Chen Y-L, Jeng US, Lai Y-H, Sun Y-S: **Morphology and properties of Nafion membranes prepared by solution casting**. *Polymer* 2009, **50**:1764–1777, https://doi.org/10.1016/j.polymer.2009.01.060.

59. Kim YS, Welch CF, Hjelm RP, Mack NH, Labouriau A, Orler EB: **Origin of toughness in dispersion-cast Nafion membranes**. *Macromolecules* 2015, **48**:2161–2172, https://doi.org/10.1021/ma502538k.

60. * Berlinger SA, Dudenas PJ, Bird A, Chen X, Freychet G, McCloskey BD, Kusoglu A, Weber AZ: **Impact of dispersion solvent on ionomer thin films and membranes**. *ACS Appl Polym Mater* 2020, **2**:5824–5834, https://doi.org/10.1021/acsapm.0c01076.
Uses *in situ* scattering techniques to understand the influence of dispersion solvent on the evolution of thin film morphology during drying and its impact of final thin film and membrane structure and properties.

61. Dudenas PJ, Kusoglu A: **Evolution of ionomer morphology from dispersion to film: an in situ X-ray study**. *Macromolecules* 2019, **52**:7779–7785, https://doi.org/10.1021/acs.macromol.9b01024.

62. Shukla S, Bhattacharjee S, Weber AZ, Secanell M: **Experimental and theoretical analysis of ink dispersion stability for polymer electrolyte fuel cell applications**. *J Electrochem Soc* 2017, **164**:F600–F609, https://doi.org/10.1149/2.0961706jes.

63. * Malek K, Eikerling M, Wang Q, Navessin T, Liu Z: **Self-organization in catalyst layers of polymer electrolyte fuel cells**. *J Phys Chem C* 2007, **111**:13627–13634, https://doi.org/10.1021/jp072692k.
Important initial molecular dynamics simulation of the ink ionomer/particle aggregation process.

64. * Mashio T, Ohma A, Tokumasu T: **Molecular dynamics study of ionomer adsorption at a carbon surface in catalyst ink**. *Electrochim Acta* 2016, **202**:14–23, https://doi.org/10.1016/j.electacta.2016.04.004.
Molecular dynamics simulation focused specifically on the ink ionomer/carbon interaction and how that interaction is modulated by solvent environment and EW.

65. Berlinger SA, McCloskey BD, Weber AZ: **Probing ionomer interactions with electrocatalyst particles in solution**. *ChemRxiv* 2021, https://doi.org/10.26434/chemrxiv.14096990.v1.

66. Thoma M, Lin W, Hoffmann E, Sattes M, Segets D, Damm C, Peukert W: **A simple and reliable method for studying the adsorption behavior of Aquivion® ionomers on carbon black surfaces**. *Langmuir* 2018, **34**:12324–12334, https://doi.org/10.1021/acs.langmuir.8b02726.

67. * Masuda T, Sonsudin F, Singh PR, Naohara H, Uosaki K: **Potential-dependent adsorption and desorption of perfluorosulfonated ionomer on a platinum electrode surface probed by electrochemical quartz crystal microbalance and atomic force microscopy**. *J Phys Chem C* 2013, **117**:15704–15709, https://doi.org/10.1021/jp404376t.
Investigates the ionomer/platinum interaction and how it changes under applied potential.

68. Kendrick I, Kumari D, Yakaboski A, Dimakis N, Smotkin ES: **Elucidating the ionomer-electrified metal interface**. *J Am Chem Soc* 2010, **132**:17611–17616, https://doi.org/10.1021/ja1081487.

69. Liu C, Uchiyama T, Nagata N, Arao M, Yamamoto K, Watanabe T, Gao X, Imai H, Katayama S, Sugawara S, *et al.*: **Operando X-ray absorption spectroscopic study on the influence of specific adsorption of the sulfo group in the perfluorosulfonic acid ionomer on the oxygen reduction reaction activity of the Pt/C catalyst**. *ACS Appl Energy Mater* 2021, **4**:1143–1149, https://doi.org/10.1021/acsaem.0c02326.

70. Fan L, Wang Y, Jiao K: **Oxygen permeation resistances and routes in nanoscale ionomer thin film on platinum surface**. *J Electrochem Soc* 2021, **168**, 014511, https://doi.org/10.1149/1945-7111/abdd7d.

71. Muzaffar T, Kadyk T, Eikerling M: **Physical modeling of the proton density in nanopores of PEM fuel cell catalyst layers**. *Electrochim Acta* 2017, **245**:1048–1058, https://doi.org/10.1016/j.electacta.2017.05.052.

72. Garrick TR, Moylan TE, Yarlagadda V, Kongkanand A: **Characterizing electrolyte and platinum interface in PEM fuel cells using CO displacement**. *J Electrochem Soc* 2016, **164**: F60–F64, https://doi.org/10.1149/2.0551702jes.

73. Devivaraprasad R, Masuda T: **Solvent-dependent adsorption of perfluorosulfonated ionomers on a Pt(111) surface using atomic force microscopy**. *Langmuir* 2020, **36**:13793–13798, https://doi.org/10.1021/acs.langmuir.0c02023.

74. Tesfaye M, MacDonald AN, Dudenas PJ, Kusoglu A, Weber AZ: **Exploring substrate/ionomer interaction under oxidizing and reducing environments**. *Electrochem Commun* 2018, **87**: 86–90, https://doi.org/10.1016/j.elecom.2018.01.004.

75. Tesfaye M, Kushner DI, Kusoglu A: **Interplay between swelling kinetics and nanostructure in perfluorosulfonic acid thin-films: role of hygrothermal aging**. *ACS Appl Polym Mater* 2019, **1**:631–635, https://doi.org/10.1021/acsapm.9b00005.

76. Modestino MA, Kusoglu A, Hexemer A, Weber AZ, Segalman RA: **Controlling Nafion structure and properties via wetting interactions**. *Macromolecules* 2012, **45**:4681–4688, https://doi.org/10.1021/ma300212f.